Catalysis Today 149 (2010) 275–280

Contents lists available at ScienceDirect

Catalysis Today

journal homepage: www.elsevier.com/locate/cattod

Valorization of α-olefins: Double bond shift and skeletal isomerization of 1-pentene and 1-hexene on zirconia-based catalysts

Inés Coleto [a], Rafael Roldán [b], César Jiménez-Sanchidrián [a], Juan P. Gómez [b], Francisco J. Romero-Salguero [a,*]

[a] Departamento de Química Orgánica, Universidad de Córdoba, Campus de Rabanales, Edificio Marie Curie, Ctra. Nnal. IV, km 396, 14014 Córdoba, Spain
[b] Centro de Tecnología de Repsol, Ctra. Nnal. V, km 18, 28631 Móstoles (Madrid), Spain

ARTICLE INFO

Article history:
Available online 23 July 2009

Keywords:
Olefins valorization
Double bond shift
Skeletal isomerization
α-Olefins
1-Pentene
1-Hexene
Zirconia-based catalysts
ZrO_2–SO_4
ZrO_2–WO_x

ABSTRACT

Several catalysts consisting of Pt supported on sulfated or tungstated zirconia (one of them supported on alumina) have been characterized by different techniques, such as elemental and XRD analyses, N_2 adsorption, TPD of ammonia, TPR and H_2 chemisorption. All these catalysts were active in the transformation of two α-olefins, 1-pentene and 1-hexene, both present in most of FCC naphthas, whose conversion to internal and branched olefins is of a great interest for their use in reformulated gasolines and as intermediate chemicals. At low reaction temperatures (200–250 °C), both hydrogenation and double bond shift compete to give *n*-paraffins and internal olefins, respectively. As the temperature rises (>350 °C) the catalytic activity for the isomerization reactions increases, yielding a higher amount of internal and branched olefins. The product composition depends on the particular catalyst and reaction conditions used. The high activity of the sulfated zirconia, is remarkable and clearly indicates the participation of acid sites in these reactions.

1. Introduction

Currently, the olefin content in gasoline is limited to 18 vol.% and it may be even more restricted in the future. However, the olefin content (particularly, $C_5^=$ and $C_6^=$) in most of FCC naphthas is higher than 40 vol.%, with *n*-olefins being more than 30% of them (Fig. 1). As a consequence, different industrial processes have recently attracted a great interest for raising the value of C_5 and C_6 olefins.

Those products obtained from the isomerization of terminal and linear olefins, i.e. internal and branched olefins, are undoubtedly advantageous for their use in reformulated gasolines and as intermediate chemicals. Thus, some possible synthetic routes starting from these olefins include alkylation, etherification and polymerization, among others (Scheme 1) [1–5]. As for their use in fuels, branched isomers and internal olefins usually shows higher octane number and lower Reid vapour pressure (RVP). Thus, among C_5 olefins, 2-methyl-2-butene has a RON of 97.3 and RVP of 14.2 psi whereas 1-pentene presents values of 90.9 and 19.1 psi, respectively. Among hexenes, these values are 76.4 and 6.3 psi for 1-hexene and 92.7 and ca. 5.2 psi for 2-hexenes, respectively.

The skeletal isomerizations of olefins are known to proceed by using a number of catalysts such as different zeolites [6–18], molybdenum oxides [19,20] and Pt supported chlorinated alumina [5], among others. The double bond isomerization of alkenes is typically catalyzed by a variety of homogeneous and heterogeneous catalysts [21]. Some practical examples are the Sumitomo process for the production of 5-ethylidenebicyclo[2.2.1]hepta-2-ene, which is catalyzed by a solid base [22], and the isomerization of linoleic acid over supported metal catalysts [23].

Olefins can undergo several transformations upon contacting a catalyst. Among them, hydrogenation, cracking, oligomerization, cyclization, double bond shift and skeletal isomerizations are the main reactions. The selectivity for these processes will depend on the catalysts and reaction conditions. In this work, the transformations of two α-olefins (1-pentene and 1-hexene) are studied on five samples consisting of Pt supported on sulfated or tungstated zirconia (one of them supported on alumina), both considered as strongly acidic catalysts.

2. Experimental

The catalysts used in this work were provided by Repsol. They were synthesized by impregnation of several supports with hexachloroplatinic acid solutions (0.02–0.1 M). Sulfated zirconia, named Pt/ZrO_2–SO_4, was supplied by Sud-Chemie. Monoclinic

* Corresponding author. Tel.: +34 957212065; fax: +34 957212066.
E-mail address: qo2rosaf@uco.es (F.J. Romero-Salguero).

0920-5861/$ – see front matter © 2009 Elsevier B.V. All rights reserved.
doi:10.1016/j.cattod.2009.06.017

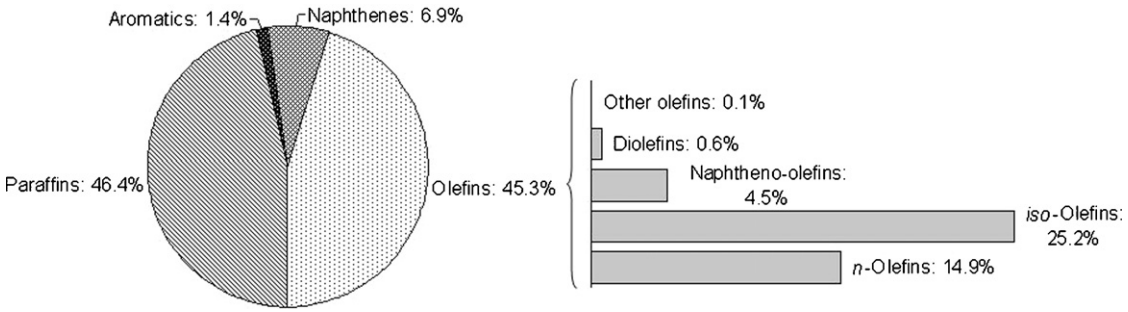

Fig. 1. Typical composition of a light FCC naphtha (wt.%) showing the content in different olefins. C_5 linear olefins account for ca. 10 wt.%.

zirconia from Saint-Gobain (ref. XZ-16052) was firstly impregnated with ammonium metatungstate (0.07 M), giving rise to the so-called catalyst $Pt/ZrO_2(m)–WO_x$. Samples $Pt/ZrO_2(t)–WO_x(1)$ and $Pt/ZrO_2(t)–WO_x(2)$ were obtained from WO_3 doped ZrO_2 (Mel Chemicals, ref. EC0110 E). Catalyst $Pt/ZrO_2–WO_x–Al_2O_3$ was prepared by previous co-impregnation of a commercial alumina (Axens ref. SPH-538) with an ammonium metatungstate (0.01 M)/zirconium acetate (3.0 M) solution. All supports were calcined in air at 500 °C for 4 h, except for $Pt/ZrO_2(t)–WO_x(2)$ at 800 °C. All impregnated samples were dried at 170 °C for 4 h and calcined in air at 500 °C for 4 h.

All catalysts were characterized by different techniques. Chemical elemental analyses were measured by X-ray fluorescence on a Phillips PW2400. X-ray diffraction patterns were recorded on a Siemens D 5000 diffractometer using Cu Kα radiation. Nitrogen adsorption isotherms were recorded on a Micromeritics ASAP 2000 analyzer. The specific surface area of each solid was determined using the BET method and the pore size distribution by the Barret–Joyner–Halenda (BJH) method. The acid properties of the catalysts were determined by temperature-programmed desorption of ammonia from 100 to 800 °C (at a heating rate of 10 °C min^{-1}) in an AutoChem-2910 equipment with a thermal conductivity detector. Previously, all samples were degassed under flowing helium at 450 °C for 1 h. TPR curves were also registered in an Autochem-2910 equipment. After being degassed at 110 °C for 1 h, the samples were analyzed from 35 to 800 °C under 50 ml min^{-1} of 10% H_2 in Ar. The metallic properties were determined by H_2 chemisorption at 35 °C in an ASAP 2000 system. Once reduced, all samples were degassed at 400 °C and 10^{-6} mbar for 4 h.

The catalytic tests were performed in a fixed-bed continuous flow reactor (10 mm i.d.) connected by a thermostated pipe to a gas chromatograph (Fisons 8000; capillary column: methyl silicone 100 m × 0.25 mm i.d. fused silica; oven program: 60–115 °C at 2 °C min^{-1}). The reactor, charged with 200 mg of catalyst, was fed at the top with the hydrocarbon mixture by means of a controlled evaporator mixer from Bronkhorst. The solids were calcined and reduced in the reactor. Calcination was done by using a N_2 stream at a flow-rate of 30 ml min^{-1} at 400 °C for 30 min, and reduction with an H_2 stream at 20 ml min^{-1} at the same temperature for 1 h. Under these analysis conditions, *n*-hexane and *trans*-3-hexene could not be discriminated. The reaction temperatures ranged from 200 to 500 °C. All reactions were conducted at atmospheric pressure.

3. Results and discussion

3.1. Characterization of the catalysts

The elemental composition and XRD patterns for all catalysts are given in Table 1 and Fig. 2, respectively. All catalysts presented platinum contents between 0.46 and 0.88 wt.%. The sulfated zirconia contained a 2.7 wt.% of sulfur. Three of the samples had WO_x species in their structure with tungsten contents ranging from 10.4 to 16.6 wt.% and another one consisted of zirconia and WO_x supported on γ-Al_2O_3. XRD analysis revealed that the so-called $Pt/ZrO_2–SO_4$, $Pt/ZrO_2(t)–WO_x(1)$ and $Pt/ZrO_2(t)–WO_x(2)$ catalysts were composed of the tetragonal phase of zirconia. On the contrary, sample $Pt/ZrO_2(m)–WO_x$, as indicated in its name, showed monoclinic zirconia. It is well established that pure zirconia is transformed from the tetragonal to the monoclinic phase at temperatures higher than 650 °C [24]. As a result of its higher calcination temperature (800 °C), solid $Pt/ZrO_2(t)–WO_x(2)$ had both tetragonal and monoclinic zirconia although the former was the main one. The dispersion and subsequent formation of small ZrO_2 crystals on solid $Pt/ZrO_2–WO_x–Al_2O_3$ made more difficult the assignment of a phase for such a compound. Nevertheless, its XRD pattern suggested the existence of tetragonal ZrO_2 supported on γ-Al_2O_3. Sample $Pt/ZrO_2(m)–WO_x$ exhibited several peaks at ca. 22–24° which can be attributed to a bulk tungsten oxide phase. These peaks were practically absent in the rest of the catalysts.

The specific surface area of zirconias is greatly influenced by the calcination temperature. Thus, Tanabe et al. [25] reported that the

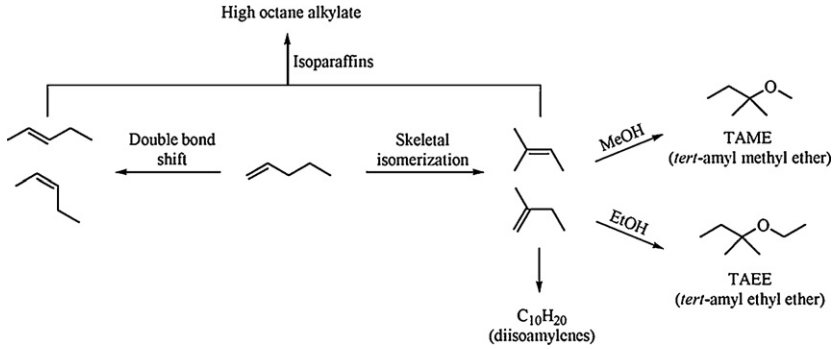

Scheme 1. Some possible processing routes starting from some C_5 olefins isomers.

Table 1
Elemental composition of the catalysts.

Catalyst	Pt (%)	Cl (%)	W (%)	S (%)	Zr (%)	Al (%)
$Pt/ZrO_2–SO_4$	0.59	–	–	2.71	–	–
$Pt/ZrO_2(t)–WO_x(1)$	0.88	0.40	12.00	–	59.01	–
$Pt/ZrO_2(t)–WO_x(2)$	0.58	–	10.40	–	61.91	–
$Pt/ZrO_2(m)–WO_x$	0.46	–	16.65	–	–	–
$Pt/ZrO_2–WO_x–Al_2O_3$	0.84	0.47	0.99	–	5.90	47.04

surface area ranged between 175.5 and 21.4 $m^2\,g^{-1}$ as the calcination temperature varied from 300 to 700 °C. Consequently, the specific surface area for sample $Pt/ZrO_2(m)–WO_x$ was the lowest among all the catalysts studied (Table 2). Moreover, samples $Pt/ZrO_2(t)–WO_x(1)$ and $Pt/ZrO_2(t)–WO_x(2)$ also showed quite different surfaces areas. Sample $Pt/ZrO_2–SO_4$ exhibited a specific surface area consistent with previously reported values [26]. Sulfate groups do not only make the transformation of phases more difficult but also increases surface area. Taking into account that the surface area for $Pt/ZrO_2–SO_4$ is 128 $m^2\,g^{-1}$ and assuming 0.25 nm^2 per sulfate group, a 2.7 wt.% S would correspond to the monolayer coverage of zirconia [26]. The pore volumes for the different samples are shown in Table 2. Catalysts containing tetragonal zirconia exhibited smaller pore volumes than samples $Pt/ZrO_2–SO_4$ and $Pt/ZrO_2–WO_x–Al_2O_3$.

The reduction of Pt species occurred below 200 °C for all the studied solids, excepting sample $Pt/ZrO_2–SO_4$, as shown in their TPR curves (Fig. 3). This catalyst exhibited an intense peak above 400 °C, which can be ascribed to the sulfate reduction enhanced by the presence of Pt [27]. The absence of a low temperature reduction peak together with the small amount of H_2 chemisorbed (Table 2) would suggest that most of Pt atoms are in an oxidized state due to strong metal support interaction in $Pt/ZrO_2–SO_4$ [28]. To a lesser extension, this phenomenon may also occur on the tungstated samples. As a consequence, Pt would lose part of its metallic character, such as reducibility and H_2 adsorption capacity. Although it is suggested that these Pt atoms would be able to activate and dissociate hydrogen [29], some authors assume that Pt atoms/clusters would be embedded in or decorated by zirconia [30], thus resulting in a lack of accessible Pt. As expected, the

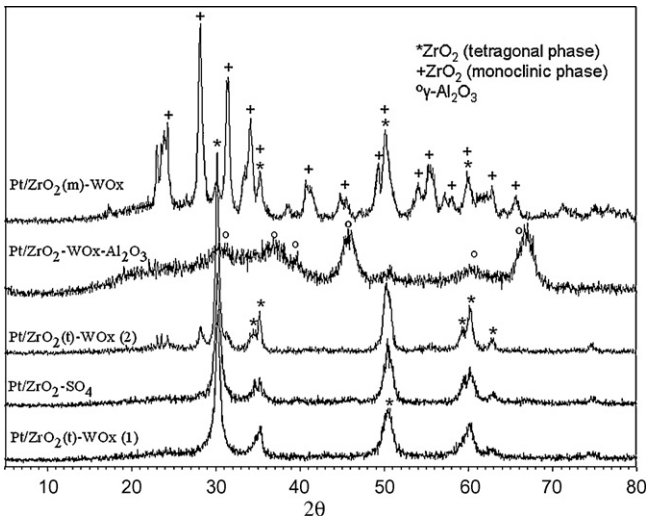

Fig. 2. Powder XRD patterns of the zirconia-based catalysts studied.

absorption capability of the solid $Pt/ZrO_2(t)–WO_x(1)$ was higher than that of the catalyst $Pt/ZrO_2(t)–WO_x(2)$, in virtue of the higher Pt content and dispersion in the former, even though they came from the same original sample but subjected to a different calcination temperature and impregnation conditions.

The ammonia TPD curves for the catalysts are depicted in Fig. 4. Their acidities were quite different. In fact, these curves indicated that samples $Pt/ZrO_2(m)–WO_x$, $Pt/ZrO_2(t)–WO_x(2)$ and $Pt/ZrO_2(t)–WO_x(1)$ were less acidic than catalyst $Pt/ZrO_2–WO_x–Al_2O_3$ and particularly $Pt/ZrO_2–SO_4$. The latter showed two peaks centred at around 150 and 470 °C, thus suggesting the predominant presence of weak and strong acid sites, respectively. It is considered a superacid solid and therefore it shows an intense desorption peak at high temperature [24].

3.2. Transformation of 1-hexene

As can be seen from Table 3, all the catalysts were active for the transformation of 1-hexene even at 250 °C. In most cases, the main

Table 2
Physicochemical properties of the catalysts.

Catalyst	Surface area ($m^2\,g^{-1}$)	Pore volume (ml g^{-1})	Pore diameter (Å)	H_2 chemisorbed (ml g^{-1})
$Pt/ZrO_2–SO_4$	128	0.27	85	0.002
$Pt/ZrO_2(t)–WO_x(1)$	113	0.07	26	0.338
$Pt/ZrO_2(t)–WO_x(2)$	43	0.08	71	0.075
$Pt/ZrO_2(m)–WO_x$	30	0.14	183	0.803
$Pt/ZrO_2–WO_x–Al_2O_3$	182	0.56	122	0.105

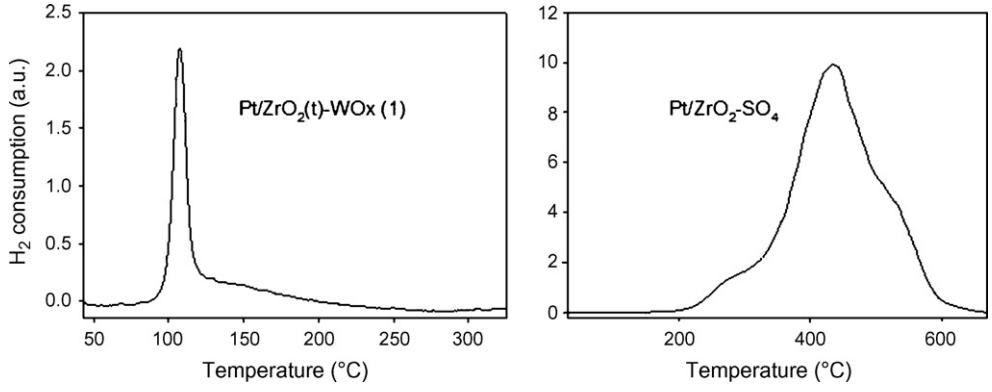

Fig. 3. TPR curves of two catalysts showing the reduction of platinum (left) or sulfate (right) species.

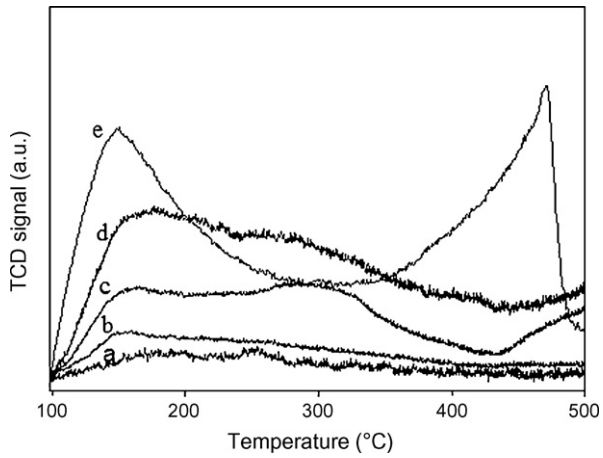

Fig. 4. Ammonia TPD curves of the catalysts $Pt/ZrO_2(m)–WO_x$ (a), $Pt/ZrO_2(t)–WO_x(2)$ (b), $Pt/ZrO_2(t)–WO_x(1)$ (c), $Pt/ZrO_2–WO_x–Al_2O_3$ (d) and $Pt/ZrO_2–SO_4$ (e).

products resulted from the double bond shift and the hydrogenation reactions, i.e. 2- and 3-hexenes and *n*-hexane, respectively. Also, small amounts of skeletal isomers, both alkanes and alkenes, were present. Even though all catalysts produced *n*-hexane in different yields, sample $Pt/ZrO_2–WO_x–Al_2O_3$ stood out because it led to the complete hydrogenation of the feed, including a small amount of isoparaffins. At this moment, any attempt to correlate the hydrogenating activity of these catalysts with the measured properties of their metallic functions has failed. On the other hand, as expected from its higher acidity, sample $Pt/ZrO_2–SO_4$ gave a higher yield to double bond isomers, i.e. 48.6% of 2-hexenes, as well as a significant amount of *n*-hexane. The rest of the catalysts showed some features in between both $Pt/ZrO_2–WO_x–Al_2O_3$ and $Pt/ZrO_2–SO_4$.

The yield to internal olefins increased at 350 °C on samples $Pt/ZrO_2(m)–WO_x$, $Pt/ZrO_2(t)–WO_x(1)$ and $Pt/ZrO_2(t)–WO_x(2)$ (Table 4). Moreover, catalyst $Pt/ZrO_2–WO_x–Al_2O_3$ still had a high hydrogenating activity, whereas solid $Pt/ZrO_2–SO_4$ decreased its production of *n*-hexane and position isomers and increased that of total skeletal isomers, being the overall yield to the latter of 18.0 wt.%. Thus, the yield to branched olefins followed the order: 2-methyl-2-pentene > *trans*-3-methyl-2-pentene > *cis*-3-methyl-2-pentene > 3-methyl-1-pentene > 2,3-dimethyl-2-butene. An increase in the reaction temperature up to 450 °C gave rise to a lower hydrogenation and a higher isomerization (both double bond shift and skeletal isomerization) activities, as shown in Table 5 for catalysts $Pt/ZrO_2(m)–WO_x$ and $Pt/ZrO_2(t)–WO_x(2)$, which exhibited quite similar results at this temperature. In all cases, cracking was hardly observed, even at 450 °C.

The *trans*-2-hexene to *cis*-2-hexene ratio in these reactions ranged from 1.8 to 2.4, whereas the thermodynamic ratios have values in between 1.1 and 1.4, depending in both cases of the temperature [31]. This fact would indicate the easier formation of the *trans* isomer in relation to the *cis* one, as well as the lack of chemical equilibrium conditions.

For comparison, the transformation of 1-hexene on several catalysts was also carried out by using N_2 as carrier gas (Table 6). These results at a reaction temperature of 350 °C revealed that both double bond shift and skeletal isomerization were less favorable under N_2 than under H_2, similarly to those obtained with supported bimetallic catalysts [5]. For instance, the yields to 2-hexenes and branched isomers for the catalyst $Pt/ZrO_2–SO_4$ decreased from 44.2% and 17.6% in H_2 to 33.0% and 2.2% in N_2, respectively. Also, the amounts of 2- and 3-hexenes were 9.9, 14.7 and 39.9 wt.% on catalysts $Pt/ZrO_2(m)–WO_x$, $Pt/ZrO_2(t)–WO_x(1)$ and $Pt/ZrO_2–SO_4$, respectively, which clearly evidence that the double bond shift is an acid-catalyzed reaction (see Fig. 4). On the other hand, the *trans*-2-hexene to *trans*-3-hexene ratios were

Table 3
Product distribution (wt.%) in the transformation of 1-hexene at 250 °C.

Compound	$Pt/ZrO_2(m)–WO_x$	$Pt/ZrO_2(t)–WO_x(1)$	$Pt/ZrO_2(t)–WO_x(2)$	$Pt/ZrO_2–WO_x–Al_2O_3$	$Pt/ZrO_2–SO_4$
Cracking (C_1–C_5)	–	–	0.3	–	–
Methylpentanes	0.1	0.9	3.4	1.2	–
1-Hexene	62.4	43.8	50.3	–	9.0
n-Hexane/*trans*-3-hexene	14.3	39.4	35.2	98.8	42.4
trans-2-Hexene	14.2	10.1	6.1	–	34.2
2-Methyl-2-pentene	–	–	0.2	–	–
cis-3-Methyl-2-pentene	0.3	0.2	0.3	–	–
cis-2-Hexene	8.0	5.3	3.1	–	14.4
trans-3-Methyl-2-pentene	0.5	0.3	0.4	–	–
Others	–	–	0.4	–	–

Reaction conditions: H_2 flow, 60 ml min^{-1}; W/F, 0.03 h; olefin flow, 7.32 g h^{-1}; H_2/olefin molar ratio, 1.7; reaction time, 60 min.

Table 4
Product distribution (wt.%) in the transformation of 1-hexene at 350 °C.

Compound	$Pt/ZrO_2(m)–WO_x$	$Pt/ZrO_2(t)–WO_x(1)$	$Pt/ZrO_2(t)–WO_x(2)$	$Pt/ZrO_2–WO_x–Al_2O_3$	$Pt/ZrO_2–SO_4$
Cracking (C_1–C_5)	0.6	0.4	0.3	0.2	2.1
3-Methyl-1-pentene	0.1	0.1	0.1	–	0.5
Methylpentanes	0.6	5.1	2.6	2.1	2.7
1-Hexene	38.1	26.6	40.8	–	7.6
n-Hexane/*trans*-3-hexene	18.6	42.8	33.2	97.4	27.9
trans-2-Hexene	25.5	15.6	14.4	–	30.9
2-Methyl-2-pentene	0.8	0.7	0.8	–	6.1
cis-3-Methyl-2-pentene	0.7	0.5	0.4	–	2.9
cis-2-Hexene	13.4	7.1	6.2	–	13.3
trans-3-Methyl-2-pentene	1.3	1.0	1.0	–	5.4
2,3-Dimethyl-2-butene	–	–	–	0.2	0.4
Others	–	0.1	0.1	–	–

Reaction conditions: see Table 3.

Table 5
Product distribution (wt.%) in the transformation of 1- hexene at 450 °C.

Compound	$Pt/ZrO_2(m)–WO_x$	$Pt/ZrO_2(t)–WO_x(2)$
Cracking (C_1–C_5)	1.6	1.6
3-Methyl-1-pentene	0.8	0.6
Methylpentanes	3.5	2.1
1-Hexene	12.6	14.7
n-Hexane/*trans*-3-hexene	16.3	17.8
trans-2-Hexene	33.7	33.9
2-Methyl-2-pentene	7.1	6.3
cis-3-Methyl-2-pentene	2.4	1.9
cis-2-Hexene	15.3	15.0
trans-3-Methyl-2-pentene	6.1	5.5
2,3-Dimethyl-2-butene	0.3	0.3
Others	0.1	0.1

Reaction conditions: see Table 3.

Table 6
Product distribution (wt.%) in the transformation of 1-hexene at 350 °C.

Compound	$Pt/ZrO_2(m)–WO_x$	$Pt/ZrO_2(t)–WO_x(1)$	$Pt/ZrO_2–SO_4$
Cracking (C_1–C_5)	0.1	–	0.2
3-Methyl-1-pentene	–	–	0.1
2-Methylpentane	–	–	0.2
1-Hexene	88.7	84.0	57.7
2-Ethyl-1-butene	0.5	0.6	–
trans-3-Hexene	1.2	2.5	6.9
trans-2-Hexene	4.9	8.1	20.3
2-Methyl-2-pentene	–	0.1	0.4
cis-3-Methyl-2-pentene	0.2	0.1	0.5
cis-2-Hexene	3.8	4.1	12.7
trans-3-Methyl-2-pentene	0.3	0.3	1.0
Others	0.6	–	–

Reaction conditions: N_2 flow, 60 ml min^{-1}; W/F, 0.03 h; olefin flow, 7.32 g h^{-1}; reaction time, 60 min.

Table 7
Product distribution (wt.%) in the transformation of 1-pentene.

Compound	$Pt/ZrO_2(t)–WO_x(1)$			$Pt/ZrO_2(t)–WO_x(2)$			$Pt/ZrO_2–WO_x–Al_2O_3$			$Pt/ZrO_2–SO_4$		
	200 °C	350 °C	500 °C	200 °C	350 °C	500 °C	200 °C	350 °C	500 °C	200 °C	350 °C	500 °C
Cracking (C_1–C_4)	–	–	–	–	–	–	–	–	0.4	–	2.4	-
3-Methyl-1-butene	–	–	–	–	–	–	–	–	0.5	–	0.9	2.2
Isopentane	0.4	2.1	–	–	–	–	0.5	1.5	1.3	–	1.8	–
1-Pentene	9.2	14.2	59.2	75.4	69.6	72.3	0.1	0.3	13.0	16.6	6.2	4.4
2-Methyl-1-butene	–	0.1	0.4	–	0.2	0.4	–	–	2.8	0.4	7.7	17.9
n-Pentane	77.6	60.4	2.6	5.1	2.8	0.5	98.3	96.0	22.2	10.2	14.0	–
trans-2-Pentene	9.0	15.0	22.8	11.8	16.6	15.5	0.6	1.4	33.0	50.8	28.6	18.7
cis-2-Pentene	3.8	7.7	12.8	6.9	9.8	9.3	0.2	0.7	17.8	19.9	13.4	8.7
2-Methyl-2-butene	–	0.4	0.7	0.4	0.6	0.8	–	–	6.0	1.9	23.3	47.7
Others	–	–	1.3	–	–	0.6	–	0.2	2.8	–	1.0	-

Reaction conditions: H_2 flow, 60 ml min^{-1}; W/F, 0.03 h; olefin flow, 7.32 g h^{-1}; H_2/olefin molar ratio, 1.4; reaction time, 60 min.

much higher (2.9–4.1) than the thermodynamic value (ca. 1.1) [31]. Since this ratio increases as the temperature decreases, it was obvious that under H_2 all solids, even $Pt/ZrO_2–SO_4$, exhibited hydrogenating activity at the lower temperatures (Table 3).

3.3. Transformation of 1-pentene

Table 7 shows the catalytic activity of several solids in the transformation of 1-pentene. In the same way as it occurred for 1-hexene, at low temperature, hydrogenation and double bond shift were the main reactions. Higher temperatures favoured the isomerization of olefins at the expense of their hydrogenation. Especially noteworthy was the high hydrogenating activity over catalysts $Pt/ZrO_2(t)–WO_x(1)$ and $Pt/ZrO_2–WO_x–Al_2O_3$, particularly at the lowest temperatures, i.e. 200 and 350 °C, as in the case of the 1-hexene transformation. All the catalysts gave rise to 2-pentenes, but the yields were highly influenced by the temperature and, as a consequence, by the competition among all the processes. Again, the *trans*-2-pentene to *cis*-2-pentene ratio (1.8–2.5) exceeded the thermodynamic ratio (1.0–1.2) [31].

Samples $Pt/ZrO_2(t)–WO_x(1)$ and $Pt/ZrO_2(t)–WO_x(2)$ exhibited a very low activity toward skeletal isomerization, and led to branched isomers (both alkanes and alkenes) with yields below 3%. In general, the most acidic catalysts, $Pt/ZrO_2–SO_4$ and $Pt/ZrO_2–WO_x–Al_2O_3$, were the most active toward the transformation of the olefin. At 500 °C, catalyst $Pt/ZrO_2–WO_x–Al_2O_3$ provided a 10.6% branched isomers. Solid $Pt/ZrO_2–SO_4$, which possessed the strongest acid sites (Fig. 4), was the most active toward total skeletal isomers accounting for 67.8% at 500 °C. The yields to branched olefins on this solid followed the order: 2-methyl-2-butene > 2-methyl-1-butene > 3-methyl-1-butene. This sequence reflects the stability of each alkene, which at the same time is related to the double bond substitution. According to the products distribution in the transformation of both 1-pentene and 1-hexene, the formation of all isoalkenes could be mainly explained by a classical unimolecular isomerization mechanism via protonated cyclopropane intermediates [10,32]. Among the six isomers of pentene, only 2-methyl-1-butene and 2-methyl-2-butene selectively react with methanol to give TAME (*t*-amyl methyl ether), which is used to boost the octane of gasoline and has a better biodegradability than MTBE (methyl *t*-butyl ether) [8]. Therefore, sample $Pt/ZrO_2–SO_4$, which gave a 65.6% of both isomers with a negligible cracking activity, is an excellent catalyst for this process, improving the results obtained with bimetallic supported chlorinated aluminas [5].

4. Conclusions

Both 1-pentene and 1-hexene can be transformed over catalysts consisting of Pt on modified ZrO_2 into different products such as paraffins, isoparaffins, internal and branched olefins depending on the particular catalyst and reaction conditions. In general, at low reaction temperatures (<350 °C), hydrogenation and double bond shift are the main reactions, whereas at higher temperatures (>350 °C) both position and skeletal isomerization reactions prevail. The most acidic catalysts, particularly sulfated zirconia, are the most active in isomerization although in some cases this is only observable at high temperature when hydrogenation hardly competes with isomerization, as occurs for the solids $Pt/ZrO_2(t)–WO_x(1)$ and $Pt/ZrO_2(t)–WO_x(2)$. At the highest temperature (500 °C), products from cracking have been negligible (<3%). It is possible to obtain yields close to 50% in 2-hexenes and 71% in 2-pentenes by using some of the catalysts studied. Even branched C_5 olefins account for 66% on the catalyst $Pt/ZrO_2–SO_4$ at 500 °C. In all cases, the amounts of branched olefins follow the same order as their stabilities. On the other hand, it has been observed that the

reactions under N_2, unlike H_2, result in a decreased activity for isomerization.

Acknowledgements

The authors wish to acknowledge funding of this research by Ministerio de Ciencia e Innovación (Project MAT2006-04847), Junta de Andalucía (Project P06-FQM-01741) and Repsol.

References

[1] V.R. Sampath, US Patent 5,649,281 (1997).
[2] F. Ancillotti, V. Fattore, Fuel Proc. Technol. 57 (1998) 163.
[3] M. Marchionna, M. Di Girolamo, R. Patrini, Catal. Today 65 (2001) 397.
[4] V.J. Cruz, J.F. Izquierdo, F. Cunill, J. Tejero, M. Iborra, C. Fité, React. Funct. Polym. 65 (2005) 149.
[5] I. Coleto, R. Roldán, C. Jiménez-Sanchidrián, J.P. Gómez, F.J. Romero-Salguero, Fuel 86 (2007) 1000.
[6] J. Abbot, A. Corma, B.W. Wojciechowski, J. Catal. 92 (1985) 398.
[7] R.A. Sawicki, R.J. Pellet, D.G. Casey, R.V. Kessler, H.-M. Huang, C.-L. O'Young, E.J. Kuhlmann, Int. J. Hydrocarbon Eng. 3 (1998) 44.
[8] T. Mäurer, B. Kraushaar-Czarnetzki, J. Catal. 187 (1999) 202.
[9] L. Domokos, M.C. Paganini, F. Meunier, K. Seshan, J.A. Lercher, Stud. Surf. Sci. Catal. 130A (2000) 323.
[10] M. Höchtl, A. Jentys, H. Vinek, Appl. Catal. A: Gen. 207 (2001) 397.
[11] D. Li, M. Li, Y. Chu, H. Nie, Y. Shi, Catal. Today 81 (2003) 65.
[12] K. Föttinger, G. Kinger, H. Vinek, Appl. Catal. A: Gen. 249 (2003) 205.
[13] F. Sandelin, I. Eilos, E. Harlin, J. Hiltunen, J. Jakkula, J. Makkonen, M. Tiitta, Stud. Surf. Sci. Catal. 154C (2004) 2157.
[14] M. Tiitta, E. Harlin, J. Makkonen, N. Kumar, D.Y. Murzin, T. Salmi, PCT Int. Appl. WO2004080590 (2004).
[15] R. Roldán, F.J. Romero, C. Jiménez-Sanchidrián, J.M. Marinas, J.P. Gómez, Appl. Catal. A: Gen. 288 (2005) 104.
[16] C. Yin, R. Zhao, C. Liu, Fuel 84 (2005) 701.
[17] H. Long, X. Wang, W. Sun, X. Guo, Catal. Lett. 126 (2008) 378.
[18] C.M. López, L. Ramírez, V. Sazo, V. Escobar, Appl. Catal. A: Gen. 340 (2008) 1.
[19] P. Wehrer, S. Libs, L. Hilaire, Appl. Catal. A: Gen. 238 (2003) 69.
[20] S. Al-Kandari, H. Al-Kandari, F. Al-Kharafi, A. Katrib, Appl. Catal. A: Gen. 341 (2008) 160.
[21] W.A. Herrmann, M. Prinz, Applied Homogeneous Catalysis with Organometallic Compounds, 2nd ed., Wiley-VCH, Weinheim, 2002.
[22] W.F. Hoelderich, Catal. Today 62 (2000) 115.
[23] A. Bernas, N. Kumar, P. Maki-Arvela, N.V. Kul'kova, B. Holmbom, T. Salmi, D.Y. Murzin, Appl. Catal. A: Gen. 245 (2003) 257.
[24] G.D. Yadav, J.J. Nair, Micropor. Mesopor. Mater. 33 (1999) 1.
[25] Y. Hakano, T. Eizuka, H. Hattori, K. Tanabe, J. Catal. 57 (1979) 1.
[26] F.R. Chen, G. Coudurier, J.-F. Joly, J.C. Vedrine, J. Catal. 143 (1993) 616.
[27] B.-Q. Xu, W.M.H. Sachtler, J. Catal. 167 (1997) 224.
[28] J.M. Grau, J.C. Yori, J.M. Parera, Appl. Catal. A: Gen. 213 (2001) 247.
[29] K. Zorn, K. Föttinger, E. Halwax, H. Vinek, Top. Catal. 46 (2007) 93.
[30] P. Lukinskas, S. Kuba, B. Spliethoff, R.K. Grasselli, B. Tesche, H. Knözinger, Top. Catal. 23 (2003) 163.
[31] S. Tsuchiya, H. Imamura, Technol. Rep. Yamaguchi Univ. 3 (1986) 399.
[32] V.B. Kazansky, Catal. Today 51 (1999) 419.